Check for updates

Received: 28 March 2024 | Revised: 18 June 2024 | Accepted: 23 June 2024

DOI: 10.1002/pc.28769

RESEARCH ARTICLE

Polymer COMPOSITES WILEY

Determination of optimum production and 3D printer application temperatures for hemp fiber reinforced polycarbonate composites

Irem Ceylan Engin[1] | **Nese Cakici Alp**[1] | **Ayse Aytac**[2,3]

[1]Department of Architecture, Kocaeli University, Architecture and Design Faculty, Kocaeli, Turkey

[2]Department of Chemical Engineering, Kocaeli University, Engineering Faculty, Kocaeli, Turkey

[3]Polymer Science and Technology Programme, Kocaeli University, Kocaeli, Turkey

Correspondence
Irem Ceylan Engin, Architecture Department, Kocaeli University, Architecture and Design Faculty, 41300 Izmit/Kocaeli, Turkey.
Email: iremceylan-@hotmail.com

Funding information
Kocaeli University Scientific Research Projects Coordination Unit, Grant/Award Number: FDK-2022-2923

Abstract

This study delves into optimizing production parameters and 3D printing (3Dp) conditions for alkaline-treated 10% hemp fiber-reinforced polycarbonate (PC) composites. Initially, composite filaments were extruded at 250°C (PCH250) and 230°C (PCH230) to assess the impact of varying melt mixing temperatures on thermal behavior. Thermal characterization was conducted using thermogravimetric analysis (TGA) and differential scanning calorimetry (DSC). DSC analysis indicated consistent glass transition temperatures (Tg) across pure PC and the composites, while TGA revealed minimal thermal degradation in PCH230 compared to pure PC. Subsequently, to ascertain the optimal 3D printing temperature, specimens were printed at temperatures elevated by 10°C relative to their melt mixing temperatures (PCH250/260 and PCH230/240), followed by mechanical evaluation via tensile testing. PCH230/240 exhibited superior mechanical properties, demonstrating a 12% increase in tensile strength and a 29% increase in Young's modulus compared to pure PC. Additional testing at 230°C printing temperature (PCH230/230) demonstrated enhanced mechanical strength over PCH250/260 but inferior performance relative to PCH230/240, attributed to incomplete interlayer adhesion observed through SEM analysis. Consequently, the optimal composite melt mixing temperature was determined to be 230°C, with an accompanying 3D printing temperature of 240°C for optimal mechanical performance.

Highlights

- 3D printable, 5% NaOH treated hemp fiber reinforced polycarbonate composite.
- Printing composite with 3D printing device at different temperatures
- 230°C process temperature gives the best thermal properties.
- 240°C 3Dp temperature provides the best mechanical and morphological properties.

This is an open access article under the terms of the Creative Commons Attribution-NonCommercial-NoDerivs License, which permits use and distribution in any medium, provided the original work is properly cited, the use is non-commercial and no modifications or adaptations are made.
© 2024 The Author(s). *Polymer Composites* published by Wiley Periodicals LLC on behalf of Society of Plastics Engineers.

KEYWORDS

3D printer materials, alkali-treated- hemp fiber, application temperatures, FDM, polycarbonate

1 | INTRODUCTION

The global environmental crisis has been caused by pollution of air, water, and soil, as well as global warming, and recycling difficulties.[1] Addressing this crisis requires minimizing environmental damage by efficiently using resources and reducing human-caused energy consumption, CO_2 emissions, and carbon footprint. The construction industry plays a significant role in this issue and is responsible for 36% of the world's energy consumption and almost 45% of its resource consumption, largely due to traditional raw materials resulting in CO_2 emissions of around 40%.[2] These negative environmental impacts are particularly critical from an architectural standpoint.

The modern understanding of architecture operates on a flat model, which unfortunately leads to the presence of polluted air, smoke, and other hazardous chemical and environmental pollutants.[1] However, to minimize environmental damage, the concept of ecological, energy-conscious, environmentally sensitive and sustainable architecture has emerged. A key tenet of sustainable architecture is the use of eco-friendly building materials and ecological construction technologies.[1] As Correia (2011) asserts, true sustainability can only be achieved when constructing with sustainable or recycled materials.[3] Due to the growing demand for eco-friendly and sustainable materials, as well as the high cost of synthetic fibers, interdisciplinary experts are collaborating to develop new natural content materials.[4]

The use of biocomposites in construction dates to the 1990s, with a focus on wood polymer composites (WPC). The historical application of lignocellulose fiber (plant fiber-based) biocomposites, however, predates this, with their introduction into the automotive industry by Henry Ford in the 1940s.[5] Among the various types of lignocellulosic biocomposites, Natural fiber-reinforced polymer composites (NFRPC) have gained attention for their durability and contribution to reducing CO_2 emissions.[6] A notable application of NFRPC within the building industry is demonstrated by the pedestrian bridge constructed by the Eindhoven University of Technology, which features a girder composed of hemp and flax fibers coupled with a polylactic acid (PLA)-based foam core.[7] The innovative application of biocomposites is exemplified in various works, such as the Tailored Biocomposite Mock-up (2019) utilizing flax fiber,[5] Dahy's (2021) load-bearing structures employing PLA, TPE, and HDPE reinforced with straw fibers,[8] Morales et al.'s (2017) architectural panel featuring PLA-reinforced bamboo fiber,[9] and Tezara et al.'s (2021) use of NFRPCs formed with jute fibers for non-structural indoor applications.[10] Further research by Dzalto et al. (2015) and Nambiyanna et al. (2021) has expanded the application of biocomposites containing flax, jute, and coir fibers for structural uses and in minimizing crack formation in building slabs.[11,12] The approach of 'Materials as a design tool', advocated by Dahy (2019), signifies a shift in architectural design toward creating structures based on material properties rather than fitting materials into predetermined designs.[13] This approach has enabled the use of natural fibers in complex structures, ushering in a new era of applying biocomposites in architecture.

Achieving complex forms in NFRPCs through design can be challenging using traditional production techniques. However, additive manufacturing (AM) offers a bottom-up approach that enables the creation of intricate structures. AM technologies include spraying a binder into a polymeric powder, using an ultraviolet laser to harden a photosensitive polymer, melting a polymeric powder with a laser (laser sintering), and fused deposition modeling (FDM).[14] Powder- and liquid-based 3D printers can cause surface elevations and distortions when used with natural fibers of light density due to buoyancy,[15] while FDM provides a sustainable and versatile solution that doesn't rely on lasers.[16] With FDM, complex prototypes and structures with good resolution can be produced quickly and cost-effectively, using a solvent-free method that involves melting and forming the polymer filament.[17] CAD programs are used to design 3D objects for FDM printing, while printer parameters (extruder geometry, processing, and structure) can be adjusted using 3Dp programs on a computer. The use of electric devices in the process makes it emission-free.[18,19] Compared to traditional manufacturing techniques, 3D printing reduces production time by almost 70%, labor costs by approximately 80%,[20] raw material usage by 70%, and waste materials by 60%.[21] This highlights how NFRPCs, and 3D printing technology can contribute to sustainable architecture and design freedom.

While utilizing NFRPCs in FDM technology has its benefits, some challenges arise during production and application. One major concern is the potential degradation of natural fibers due to the production process's required temperature. Most natural fibers begin to break

15480569, 0, Downloaded from https://4spepublications.onlinelibrary.wiley.com/doi/10.1002/pc.28769 by Turkey Cochrane Evidence Aid, Wiley Online Library on [11/07/2024]. See the Terms and Conditions (https://onlinelibrary.wiley.com/terms-and-conditions) on Wiley Online Library for rules of use; OA articles are governed by the applicable Creative Commons License

down when exposed to conditions above 200°C for extended periods.[22] When considering the use of NFRPC materials in 3D printing for architectural purposes, they are exposed to high temperatures during both the preparation of the filament composite material and the printing phase. The printing temperature plays a crucial role in controlling viscosity and should be high enough to allow for easy flow through the nozzle while not interfering with layer bonding.[18] The mechanical properties of 3D printed objects are influenced by the material's characteristics, layer bonding, and adjacent path propagation. The bond quality between layers is heavily impacted by production parameters such as temperature profile, and poorly bonded layers can decrease mechanical properties.[23] McIlroy and Olmsted (2017) found that varying printing speed, temperature, and the number of entanglements had differing effects on polymer composite properties.[24]

This research aims to enhance sustainable architecture by studying the ideal application temperatures for NFRPC's used in 3D printing with a focus on FDM. The study highlights the preference for thermoplastics as matrix materials due to their superior dehumidification characteristics, which improve layer adhesion during the 3D printing process.[25–27] The investigation reviews existing literature on thermoplastic-based NFRPC filaments developed for 3D printers, encompassing a variety of natural fibers such as rice straw,[28,23] jute,[29,30] gongura roselle,[31] coconut,[32] oil palm,[33] and royal palm fibers[34] reinforced with Acrylonitrile Butadiene Styrene (ABS). Similarly, Polylactic Acid (PLA) has been utilized alongside jute,[35] Henequen,[6] agave,[37] sugarcane bagasse,[38] bamboo,[16] and hemp fibers.[39] Flax,[40] hemp,[41] and harakeke[42] fibers have been used as reinforcements for polypropylene (PP). Poly-butylene succinate (PBS) has been used by flax,[43] hemp,[44] and coconut fiber,[45] whereas there are studies on expanded polystyrene foam (EPS) and corn husk fibers.[46] In this research, the focus is on selecting thermoplastic materials compatible with 3D printing technology and commercially available in filament form. These materials are ABS, Polycarbonate (PC), and PLA.[47] PC is of particular interest due to its amorphous nature, 3D printability, and wide industrial applications, especially in architecture and construction. This research posits that despite the extensive industrial applications of PC, there is a notable gap in the literature on its reinforcement with natural fibers for use in FDM technology. This study aims to fill this gap by proposing a sustainable material alternative that maintains the mechanical properties of PC and is suitable for 3D printing applications.

When it comes to NFRPC filaments, the strength of the 3D printed product is dependent on the type of plant fiber used.[48] Hemp and flax plants are renowned for providing greater stability, thanks to the bast fibers in their structure, and have better strength than fruit fibers.[49] Flax fibers, on the other hand, are mostly composed of low-molecular-weight pectin and cannot participate in charge transfer due to their rough structure, making them a potential surface defect.[50,51] Thus, it was deemed more appropriate to use hemp fiber to prevent surface defects that may occur during 3D printing. Hemp fiber is beneficial for sustainable architecture due to its faster growth rate and higher CO_2 absorption capacity than any other existing plant.[52] In our previous study, the chemical, thermal, mechanical, and morphological properties of PC composites were investigated and reinforced with different hemp fiber ratios. It was found that 10 wt% hemp content is the optimal ratio for reinforcing the PC matrix.[53] Therefore, in this paper, a fixed hemp fiber content of 10 wt% was used.

When using composites reinforced with natural fibers, some challenges arise due to the hydrophilic nature of these fibers. Some of these challenges include weaknesses in the bond between the fibers and the matrix, and moisture uptake. To overcome these issues, various chemical treatments are performed on the surface of the fibers, such as alkaline, and silane treatments. These treatments help to strengthen the bond between the fibers and the polymers, reduce moisture uptake, and improve resistance to microbial degradation.[54] Hemp fibers are known to be highly hydrophilic and contain 4%–16% hemicellulose, 2%–5% lignin, and 0.8%–8% pectin, making the fibers coarse and stiff.[55,51,56] However, according to research, the most effective treatment for hemp fibers is the NaOH alkaline treatment.[57,58–60] This treatment removes certain compounds from the fibers and increases the hardness of the fiber surface, resulting in a better bond with the matrix material.[57] Additionally, hemp fibers that have undergone this treatment show improved thermal resistance and surface hardness.[60,61] The goal of this study is to determine the best production and application temperatures for a PC composite that is reinforced with 5% NaOH alkali-treated hemp fibers.

The effects of different temperatures on the mechanical, thermal, and morphological properties of the composite were investigated in this study. For this purpose, thermal properties of the composites were determined by using TGA and DSC analyses, mechanical properties were determined by tensile testing, and morphological properties were determined by SEM analysis. As a result, the findings of this study tried to support sustainable architecture by increasing the performance of composites reinforced with natural fibers.

15480569, 0, Downloaded from https://4spepublications.onlinelibrary.wiley.com/doi/10.1002/pc.28769 by Turkey Cochrane Evidence Aid, Wiley Online Library on [11/07/2024]. See the Terms and Conditions (https://onlinelibrary.wiley.com/terms-and-conditions) on Wiley Online Library for rules of use; OA articles are governed by the applicable Creative Commons License

2 | EXPERIMENTAL

2.1 | Materials

The Pure PC was used as the control sample while Lotte Chemical provided the matrix material that is suitable for general use. This material has a tensile strength of 63–70 MPa, elastic modulus of 2400–2500 MPa, deformation temperature of 130°C, vicat softening temperature of 150°C, and a fluidity index (MFI) of 10. The hemp fibers were sourced from Hemp Traders of America in their raw form, degummed, and with lignin not removed. The sodium hydroxide (NaOH) used in the experiment was obtained from Katki Dunyasi and has a purity of 99%.

2.2 | Methods

In this study studied different temperatures during the production and 3Dp application phases of PC composite filaments reinforced with alkaline treated 10 wt% hemp fiber, and the samples with the most optimum thermal and mechanical results were determined. The temperatures studied for the melt mixing process are 250°C and 230°C, and the sample with the thermal degradation resistance was determined by TGA and DSC analyses. The samples were printed on an Anycubic I3 Mega device with a printing temperature 10°C higher than their melt mixing temperature. The 3Dp temperatures are 260°C and 240°C.

2.3 | Composite preparation

The hemp fibers selected for use in the composite within the scope of the study were cut into 6-mm lengths and subjected to alkaline treatment with 5% NaOH/pure water solution at 120°C to remove surface roughness, improve thermal resistance, and form a better interfacial bond with the PC matrix. The hemp fibers were alkaline treated and then washed with tap water until the pH was neutral and subjected to dehumidification at −0.6 bar pressure and 80°C for 24 h. The exact drying process was applied to the PC granules. The dried fibers and PC granules were weighed at a ratio of 10/90 Hemp/PC and fed in a laboratory-scale co-rotating twin-screw mini extruder (Xplore 15 mL Micro-compounder). The materials were fed into the laboratory-scale twin screw extruder device with the help of the feed hopper and mixed using the melt mixing method. The mixing time was 4 min and hemp fibers were added in the last 1 min. The device was operated at two different temperatures, 250°C and 230°C to obtain composites (see Table 1). The composite material from the nozzle of the extruder device was shaped in filament form with the help of a conveyor belt to be suitable for use in the 3D printer. The samples were named PCH250 and PCH230. The flowchart showing the production process of composite filaments is in Figure 1.

TABLE 1 Melt mixing process parameters of the composite samples.

Sample	PC (%)	Hemp Fiber (%)	Extruder Temperature (°C)	Mixing Time (min)
PCH250	90	10	250	4
PCH230	90	10	230	4

First, the aim was to investigate the mechanical properties when the 3Dp nozzle temperature was 10°C higher than the extruder mixing temperature. Both PCH250 and PCH230 samples were printed with a nozzle temperature 10°C higher than the extruder mixing temperature, and the sample with the best mechanical result was separated for use in the next test phase. Then, the aim was to investigate the mechanical properties of the sample when the 3Dp nozzle temperature was 10°C lower than the extruder mixing temperature. However, because the PC polymer matrix material had a yielding problem at a nozzle temperature lower than 230°C, the lowest nozzle temperature was set at 230°C. The PCH230 sample with the best thermal and mechanical properties was printed at a printer temperature of 230°C and compared with the 240°C printed sample. Thus, the optimum production and application conditions for the PC matrix reinforced with 10 wt% hemp fiber were determined. Based on the TGA results, pure PC can remain intact up to approximately 430°C. The print temperature for the control sample of pure PC was 260°C. The printed samples were named PCH250/260, PCH230/240, and PCH230/230. The FDM deposition angle is −45°/45° and 0°/90°. Figure 2 shows an illustration of the 3D printing stage of composite filaments. The extruder temperature, print temperature, and bed temperature values of the samples are given in Table 2. The parameters except print temperature are the same for all samples and are given in Table 3.

2.4 | Characterization

This study applied thermogravimetric analyses (TGA) tests to composite filament samples obtained by the melt

15480569, 0, Downloaded from https://4spepublications.onlinelibrary.wiley.com/doi/10.1002/pc.28769 by Turkey Cochrane Evidence Aid, Wiley Online Library on [11/07/2024]. See the Terms and Conditions (https://onlinelibrary.wiley.com/terms-and-conditions) on Wiley Online Library for rules of use; OA articles are governed by the applicable Creative Commons License

mixing method at two different temperatures, pure PC filament and 5% NaOH-treated hemp fibers (T.Hemp fibers). The data was verified by repeating the TGA analysis twice. The TGA analysis was performed using the Mettler Toledo MTTA18110856 TGA 1 under a nitrogen atmosphere. The testing was conducted within a temperature range of 25°C to 600°C, with a heating rate of 10°C/min and a 30 mL/min nitrogen flow. The samples, weighing approximately 10 mg, were placed in a ceramic pan within the device.

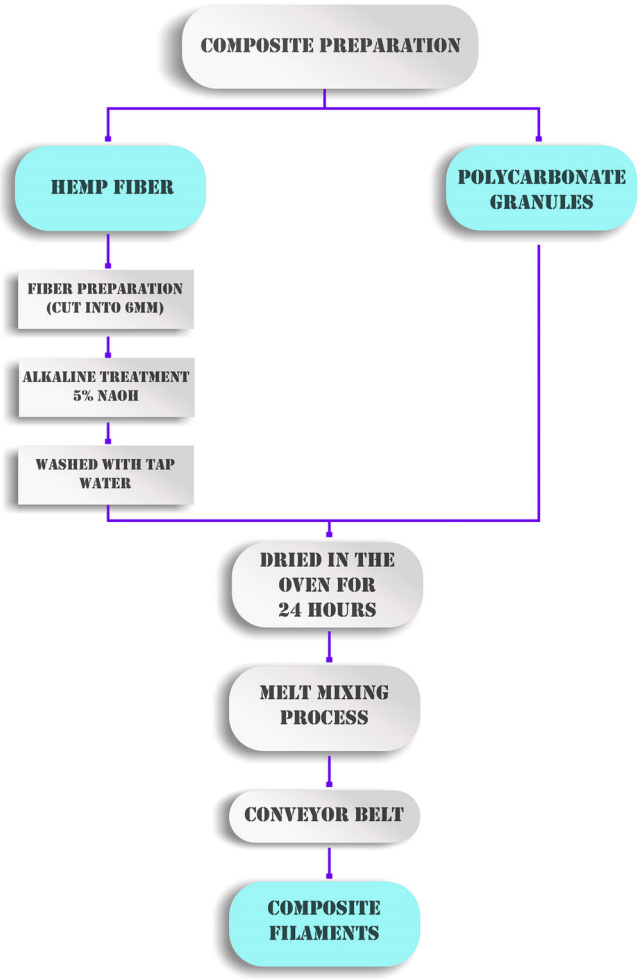


FIGURE 1 Production process of composite filaments.

TABLE 2 Print and bed temperatures of the pure PC and composite samples.

Sample	Extruder temperature (°C)	3Dp printing temperature (°C)	3Dp bed temperature (°C)
PC	250	250	110
PCH250/260	250	260	110
PCH230/240	230	240	110
PCH230/230	230	230	110

TABLE 3 3D printing parameters of the composite samples.

3D printing parameters	
First layer height (mm)	0.3
Layer height (mm)	0.1
Layer width (mm)	0.4
Filling pattern	Line
Filling ratio (%)	100
Fill alignment (degree, angle)	45
Shell thickness (mm)	1.0
Number of shells	2
Printing speed (mm/s)	35.0
Nozzle diameter (mm)	1.0

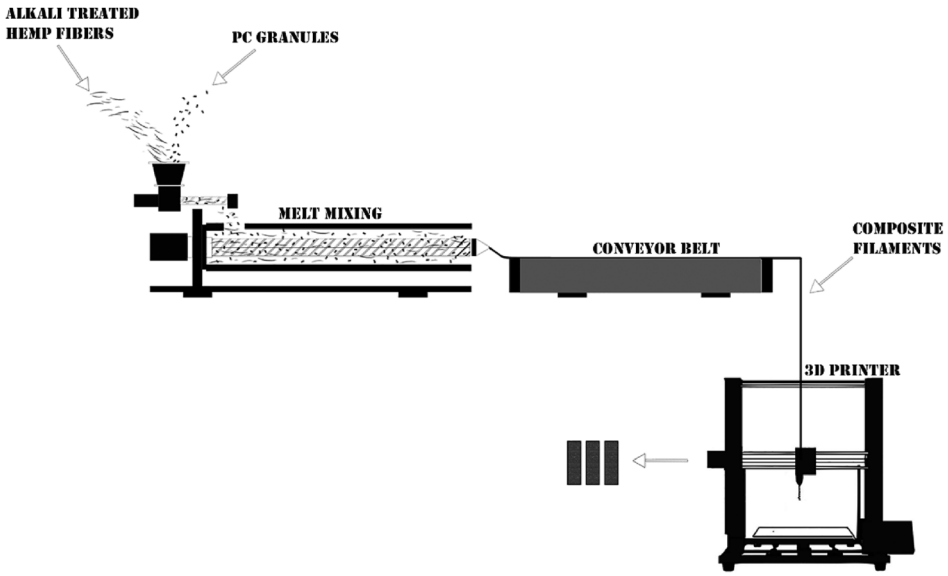


FIGURE 2 Illustration of the 3D printing of composite filaments.

15480569, 0, Downloaded from https://4spepublications.onlinelibrary.wiley.com/doi/10.1002/pc.28769 by Turkey Cochrane Evidence Aid, Wiley Online Library on [11/07/2024]. See the Terms and Conditions (https://onlinelibrary.wiley.com/terms-and-conditions) on Wiley Online Library for rules of use; OA articles are governed by the applicable Creative Commons License

Differential scanning calorimetry (DSC) analysis was applied to composite filament samples obtained by melt mixing at two different temperatures, pure PC filament and 5% NaOH- treated hemp fibers (T.Hemp fibers). To ensure the accuracy of the results, the DSC analysis was repeated twice. A Mettler Toledo DSC machine with nitrogen gas was used for the analysis. The analysis has a two-stage method with a 10°C/min temperature increase between 25 and 250°C. After heating the samples from 25°C to 250°C, cooled them down to 25°C and then increased the temperature to 250°C. During the first heating stage, the thermal traces left by the twin-screw extruder were eliminated, and the results of the second heating stage were considered. By performing this analysis, the T_g values of the samples are determined.

The tensile strength and Young's modulus values were examined in the tensile test. In architectural applications, it is crucial to consider the mechanical values of tensile strength and Young's modulus. Within the scope of the study, both tensile and Young's modulus tests were applied to three bars of $75 \times 12 \times 2mm^3$ from each composite specimen and pure PC specimen. The tests were conducted using an Instron Tensile Machine with 6 bar pressure and the Instron Bluehill Universal program with the ISO 527-5 A 10 mm/min method. Moreover, their mechanical properties were determined.

The morphology of the produced composite samples was determined using an electron microscope SEM, Quanta FEG 450 device. The SEM analysis was performed using the device in the secondary electron mode under 15.00 kV current and 44.8 GPa pressure. The zoom ratios of 100, 500, and 1000 were used to observe the samples. The samples analyzed in the SEM were obtained from composite samples produced by the FDM technique and subjected to tensile tests. The gold plating was applied to the specimens for 90 seconds under a voltage current of 10 mA to enable conductivity in the polymer-containing insulating materials.

3 | RESULTS AND DISCUSSION

3.1 | Thermogravimetric analysis

The thermogravimetric analysis (TGA) and derivative weight (DTG) curves of the composite samples are shown in Figure 3, the heat-induced mass loss values are summarized in Table 4, and the DTG values are summarized in Table 5. Looking at the TGA graph, three peaks appear for hemp fibers alkaline treated with 5% NaOH. The first occurred at 94.20°C and is 5% weight loss. Looking at the literature's TGA analysis of hemp fibers alkaline treated with NaOH in the literature, Rachini (2009) determined the peak value as 87°C for approximately 5% mass loss.[59] Approximately 6%–8% weight loss is attributed to inherent moisture in the fiber, and the results of the TGA analysis performed in this study approximately coincide with the results in the literature. The difference of about 7°C between the studies in the literature is thought to be related to the alkaline treatment rate applied in this study and the drying conditions applied to the fibers, and it can be said that the moisture content in the fibers is reduced to a lesser extent. The first DTG peak occurs at approximately 60°C. This DTG peak is like that reported in the literature and is attributed to moisture loss.[62] At the second DTG peak, it is seen that while there is 10% mass loss at 311°C, the loss is 50% at 358°C. With the second peak formed between these temperatures, the fiber deteriorates rapidly. The second peak is attributed to hemicellulose, lignin, and cellulose degradation. Hemicellulose degrades at 300°C, lignin starts at 300°C and degrades at 450°C, and cellulose starts at 275°C and degrades completely at approximately 550°C.[63] Upon review the literature, it is observed that hemp fibers subjected to alkali treatment exhibit a rapid onset of deterioration commencing at 303°C. Notably, a significant weight loss of 50% is observed at approximately 359°C.[62] In another study, it starts to deteriorate rapidly after 250°C and completely deteriorates at 350–360°C.[63] Consequently, the TGA of NaOH-alkaline-treated hemp fibers observed in this investigation aligns with findings documented in the extant scholarly literature.

The TGA analysis of the pure PC sample shows that it has a single degradation peak. After 478.37°C, where 10% weight loss temperature of the PC sample occurred, there was a rapid decrease and the degradation of the polymer accelerated. Upon examining the specimens denoted as PCH250 and PCH230, to which hemp fiber was incorporated, it is observed that there is a discernible reduction in thermal strength relative to the specimen composed solely of pure PC. The lower residue levels in samples associated with PCH250 and PCH230 can be attributed to the early combustion of fibers compared to PC. A comparison of pure PC and hemp fibers at 600°C indicates that the residual amount of T. hemp fibers is 15.73%, while pure PC has a residue amount of 26.52%. This pattern is also observed in composite samples. In the literature, the composite obtained using PC and fruit fibers[64] and the pineapple leaf fiber-reinforced PC composite[65] show similar results. The addition of natural fibers to PC, a polymer that degrades at high temperatures, decrease its thermal degradation temperature. A similar situation is observed in PP and PES thermoplastics reinforced with hemp fiber.[62]

The TGA analysis of the PCH250 and PCH230 samples showed that 10% weight loss occurred at 425.53°C in the PCH250 sample and 431.40°C in the PCH230 sample.

15480569, 0, Downloaded from https://4spepublications.onlinelibrary.wiley.com/doi/10.1002/pc.28769 by Turkey Cochrane Evidence Aid, Wiley Online Library on [11/07/2024]. See the Terms and Conditions (https://onlinelibrary.wiley.com/terms-and-conditions) on Wiley Online Library for rules of use; OA articles are governed by the applicable Creative Commons License

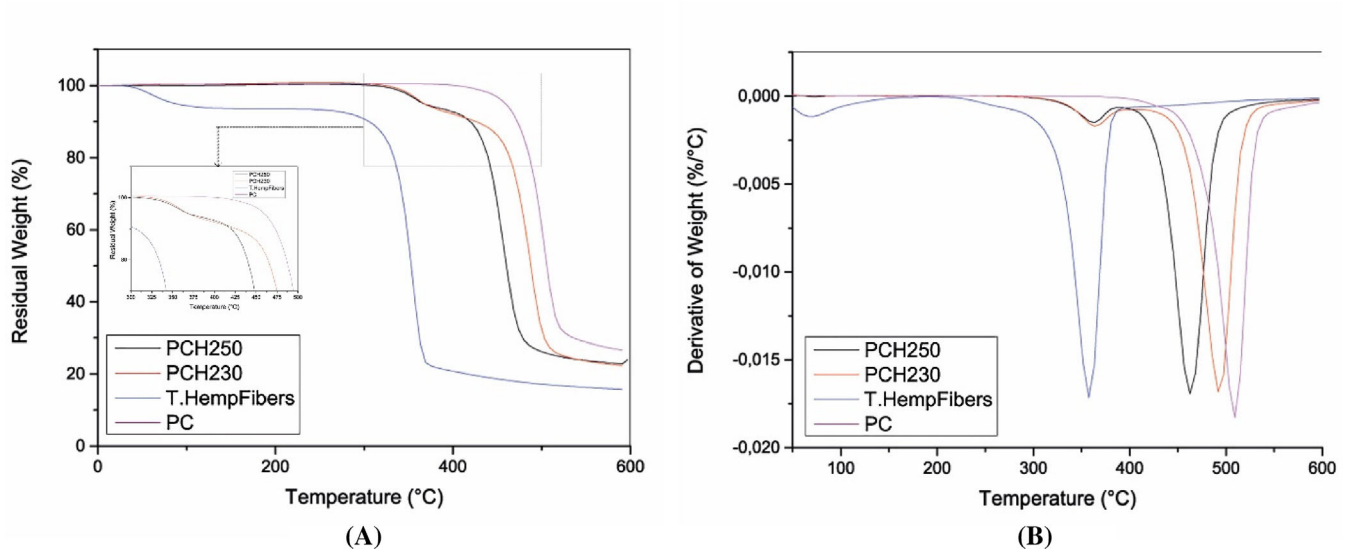


FIGURE 3 Thermogravimetric analysis (TGA) (A) and derivative weight (DTG) (B) thermograms of the composites.

TABLE 4 Heat-induced mass loss due to the TGA analysis of composite samples.

Sample	5% weight loss temp. (°C)	10% weight loss temp. (°C)	50% weight loss temp. (°C)	600°C residue (%)
T.Hemp fibers	94.20	311.01	358.84	15.73
PC	465.37	478.37	511.51	26.52
PCH250	373.10	425.53	466.21	22.73
PCH230	373.10	431.40	493.47	22.21

TABLE 5 DTG peaks of the composite samples.

	PC	PCH250	PCH230
T_{max} (°C)	508.57	463.27	493.47

This indicates that the fibers processed at 230°C extruder temperature are less damaged in the melt mixing stage than those processed at 250°C and can maintain their mass and a higher thermal degradation temperature is obtained. Although the PCH230 sample seems to lose weight at higher temperatures, the remaining mass at 600°C is almost the same. Whether the superior properties of the PCH230 sample compared to the PCH250 sample are similar in mechanical properties has been tested by printing both samples at a printer temperature 10°C higher than the extruder temperature. Afterward, the sample with better mechanical properties will be compared by printing at a printer temperature 10°C lower than the extruder temperature. Since pure PC can remain intact at high temperatures, the printer printing temperature was set at 250°C.

When the DTG peaks of pure PC and composites are analyzed, PC and PCH230 samples give very close peak values. As a result, the melt mixing of hemp fibers used to reinforce the PC matrix at 230°C does not significantly reduce the thermal strength of pure PC.

3.2 | DSC analysis

DSC analysis was performed two stages, the first stage erased the temperature traces from the extruder device, and the T_g value results obtained from the second stage were considered. No significant differences in T_g values were detected between the pure PC, and composite filament samples. T_g values of pure PC, PCH230, and PCH250 were obtained as 148.44, 148.99, and 148.64°C, respectively. In the literature, Stelea et al. (2022) did not detect a significant decrease in the T_g values of the composite obtained by adding hemp fiber to the polyester matrix. While the T_g value of pure polyester was 77.52°C, it was 74.58°C when hemp fiber was added.[62] Baghaei et al. (2014) reinforced a PLA matrix with hemp fibers. At the same time the T_g value of pure PLA is 59.2°C, this value is 59.4°C for PLA/Hemp composite.[66] Karsli and Aytac (2014) reinforced a PLA/PC blend with flax fiber. The T_g values obtained from DSC analysis were 58.2°C

15480569, 0, Downloaded from https://4spepublications.onlinelibrary.wiley.com/doi/10.1002/pc.28769 by Turkey Cochrane Evidence Aid, Wiley Online Library on [11/07/2024]. See the Terms and Conditions (https://onlinelibrary.wiley.com/terms-and-conditions) on Wiley Online Library for rules of use; OA articles are governed by the applicable Creative Commons License

for the polymer blend and 58.5°C when adding flax fiber.[67] The Tg values obtained by adding hemp fiber to the PC matrix are like those reported in the literature.

3.3 | Mechanical characteristics

To determine the mechanical character, PCH250 and PCH230 specimens were printed with an Anycubic I3 Mega 3D printer device at a temperature 10°C higher than the extruder operating temperature. The PCH250 specimen was printed at a temperature of 260°C and was labeled as PCH250/260, while the PCH230 specimen was printed at a temperature of 240°C and was named PCH230/240. Upon analysis, it was determined that the PCH230/240 specimen with an extruder temperature of 230°C showed superior mechanical properties and was separated to be printed at temperature 10°C lower than the extruder temperature. However, it was observed that printing at a temperature of 220°C resulted in blockages and layer separation due to the melting of the PC matrix at higher temperatures. As a result, the lowest printable temperature for the PCH230 specimen was determined to be 230°C and it was printed at this temperature and labeled as PCH230/230. All composite samples well then compared to a pure PC sample printed in the same dimensions. Figure 4. displays the 3Dp printed specimens before tensile test while Figure 5 shows the same specimens after tensile test. It should be noted that slight variations in color were observed among the specimens, which were attributed to differences in extruder and printer temperatures.

The graphs illustrating the tensile strength and Young's modulus of the samples depicted in Figure 6 provide data obtained from the respective tests. Upon closer examination of the tensile strength values obtained from the test, it was observed that the PCH250/260 sample did not exhibit a significant increase when compared to the pure PC sample. The sample with the best tensile strength was PCH230/240. It was produced at 230°C extruder temperature and 240°C printing temperature. The specimen denoted as PCH230/240 exhibited an enhancement in tensile strength by approximately 12% in comparison to the control specimen of pure PC. Following closely, the specimen labeled PCH230/230 demonstrated a notable improvement, with tensile strength increasing by approximately 7% relative to the pure PC specimen. It is thought that the PCH230/240 sample has the best mechanical strength because the damage was minimized by exposing the fibers to less temperature in the extruder stage, while the nozzle temperature used in the 3Dp stage allows the layers to adhere to each other better. Interlayer adhesion

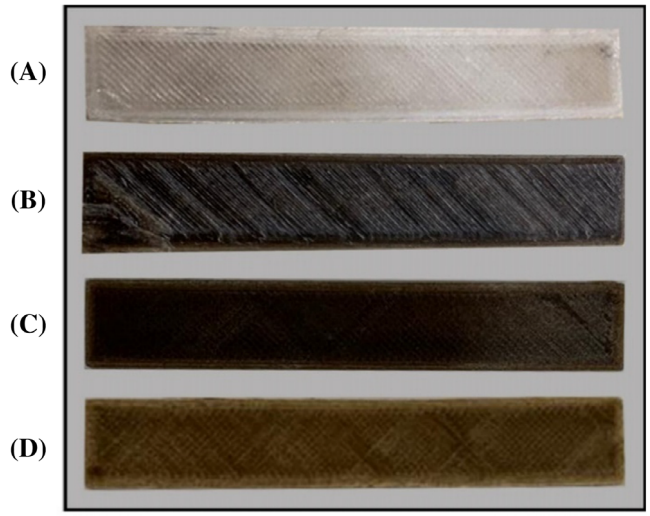


FIGURE 4 3D printed composite samples before tensile test: (A) pure PC; (B) PCH250/260; (C) PCH230/240; (D) PCH230/230.

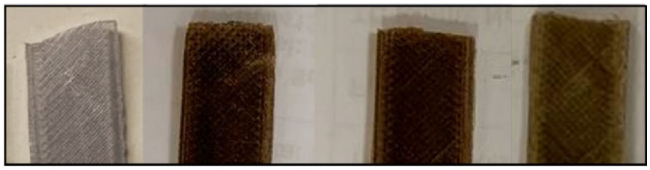


FIGURE 5 3D printed composite samples after the tensile test: (A) pure PC; (B) PCH250/260; (C) PCH230/240; (D) PCH230/230.

was examined in more detail using the images obtained from SEM analysis. The increase in tensile strength values because of the reinforcement of the PC matrix with natural fibers is like the studies in the literature. Threepopnatkul et al. (2009) observed a slight increase in tensile strength when the PC matrix was reinforced with PALF fibers.[65] Baghaei et al. (2014) achieved an approximately 15% increase in the tensile strength of PLA reinforced with hemp fiber. For the PP matrix reinforced with hemp fibers, a 9% increase was achieved compared with the pure form of the matrix material.[66]

A comparable observation can be noted in the context of Young's modulus values, wherein the specimen denoted as PCH230/240 exhibits a significantly elevated modulus value. Threepopnatkul et al. (2009) observed that when the PC matrix was reinforced with PALF fibers, the Young's modulus value increased by 75%.[65] The PCH230/240 sample showed an increase of 28% compared with the pure PC sample. This increase in both the tensile strength and Young's modulus values indicates that a good interface bond has been established between the hemp fibers and the PC matrix. While the tensile

15480569, 0, Downloaded from https://4spepublications.onlinelibrary.wiley.com/doi/10.1002/pc.28769 by Turkey Cochrane Evidence Aid, Wiley Online Library on [11/07/2024]. See the Terms and Conditions (https://onlinelibrary.wiley.com/terms-and-conditions) on Wiley Online Library for rules of use; OA articles are governed by the applicable Creative Commons License

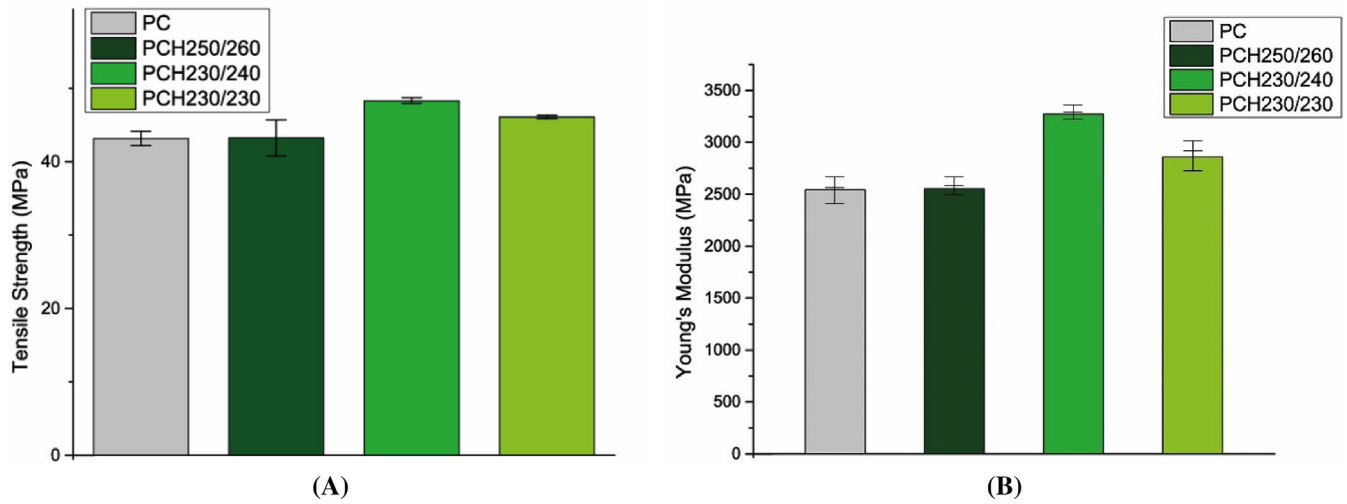


FIGURE 6 (A) Tensile strength of the composite samples; (B) Young's modulus of the composite samples.

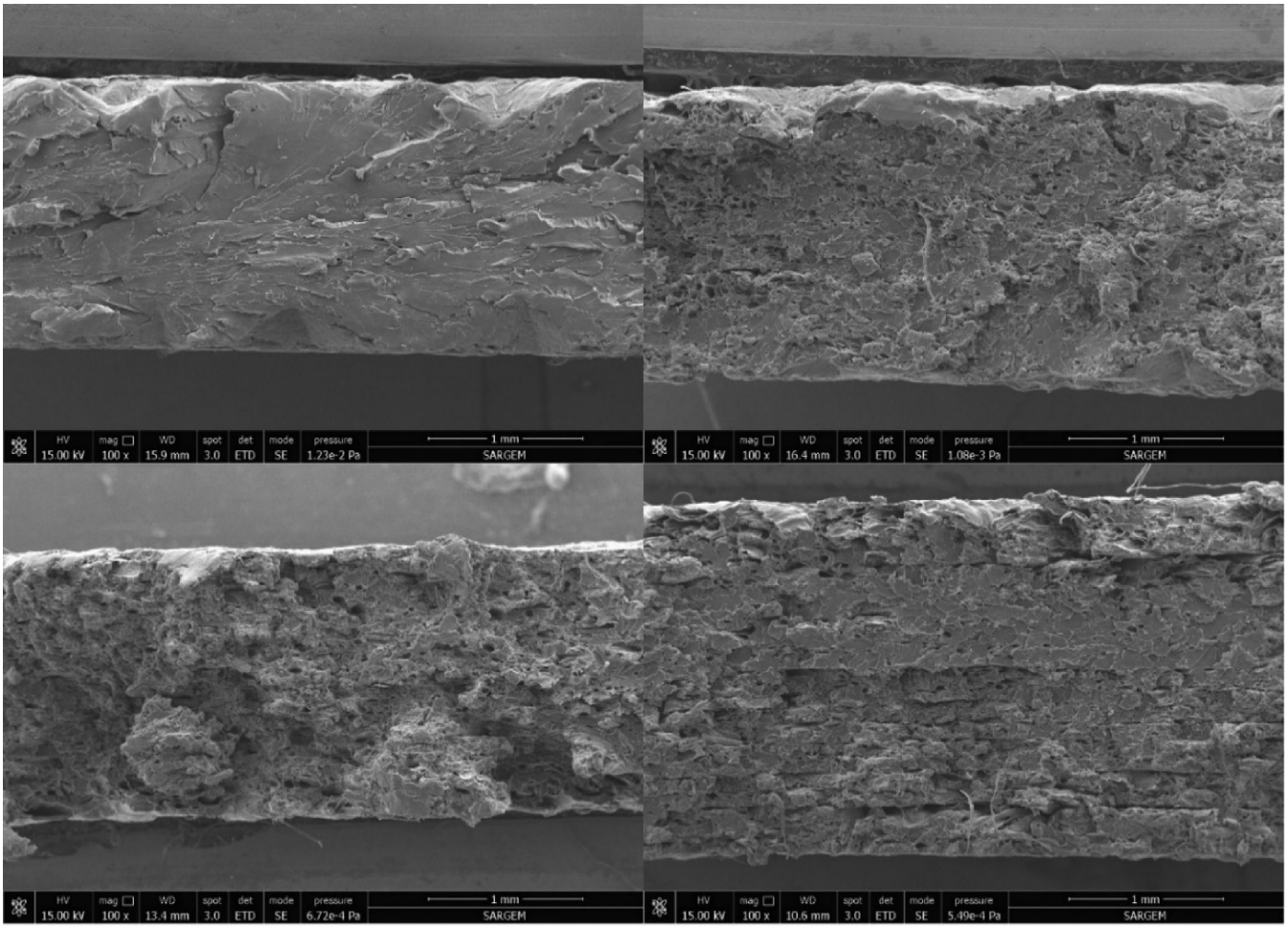


FIGURE 7 100× SEM images. (A) Pure PC; (B) PCH250/260; (C) PCH230/240; (D) PCH230/230.

strain at maximum force value was 4.78% for the pure PC sample, 4.91%, 6.41%, and 5.84% were obtained for PCH250/260, PCH230/240 and PCH230/230 samples, respectively. All composite samples observed a slight increase in tensile strain at maximum force compared with pure PC.

15480569, 0, Downloaded from https://4spepublications.onlinelibrary.wiley.com/doi/10.1002/pc.28769 by Turkey Cochrane Evidence Aid, Wiley Online Library on [11/07/2024]. See the Terms and Conditions (https://onlinelibrary.wiley.com/terms-and-conditions) on Wiley Online Library for rules of use; OA articles are governed by the applicable Creative Commons License

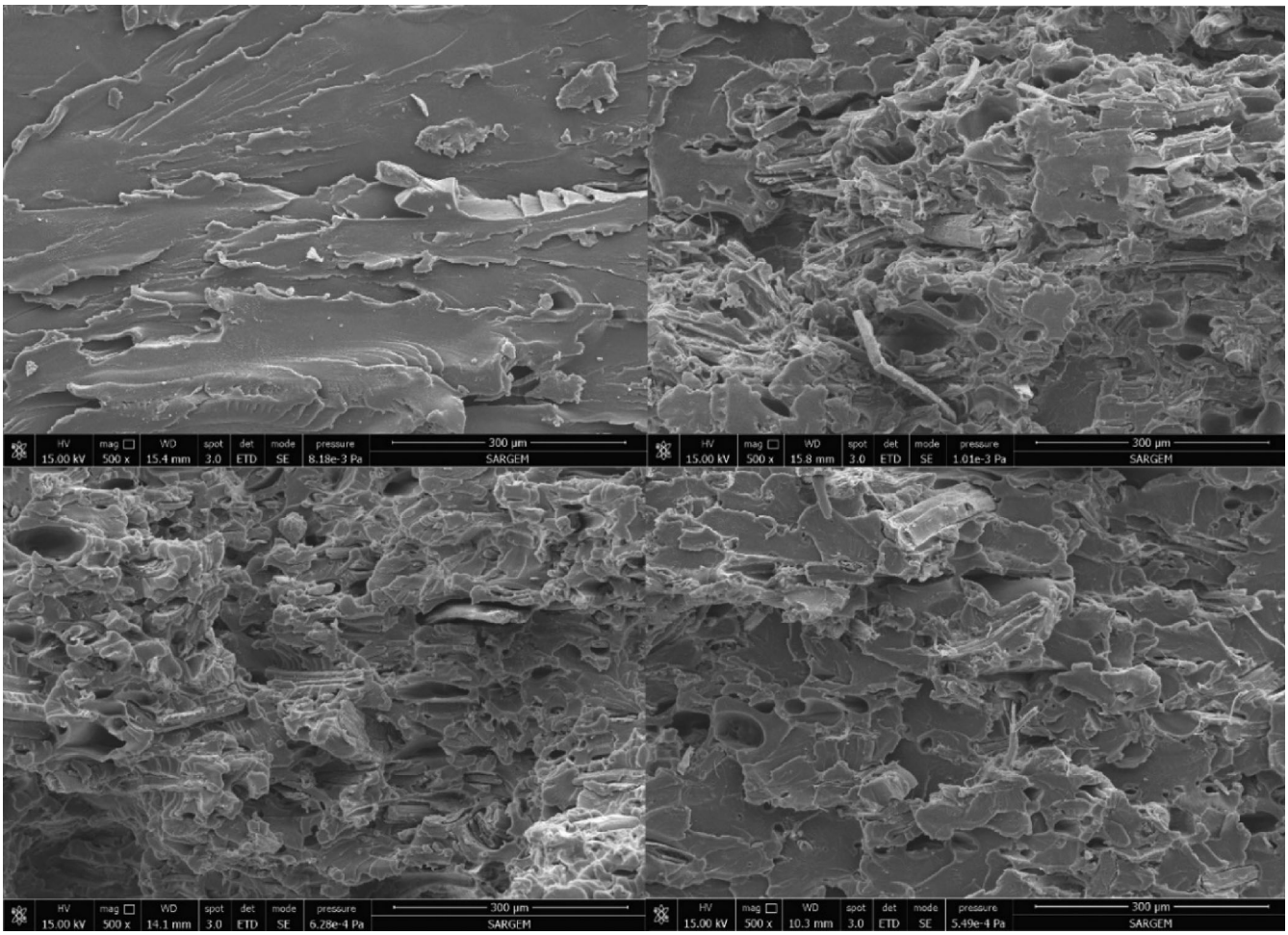


FIGURE 8 500× SEM images. (A) Pure PC; (B) PCH250/260; (C) PCH230/240; (D) PCH230/230.

3.4 | SEM analysis

SEM images taken from the fractured surfaces of the tensile test applied to pure PC, PCH250/260, PCH230/240, and PCH230/230 composites formed by the 3Dp are shown in Figures 7–9.

Upon examining the 100× scanning electron microscope (SEM) images of the fracture surfaces following the tensile testing of the 3D printed specimens, as depicted in Figure 7, it is observed that porous structures are prevalent on the surfaces of all samples. According to Zhou et al. (2020), this porous structure is attributed to the production stage using a 3Dp.[68] Upon examining the specimen labeled PCH230/230 in Figure 7D, the initial observation that commands attention is the discernible interlayer spacing. These voids are attributed to insufficient bonding and stress concentration generated at pre-existing voids formed during 3D printing.[36] Upon examination of the composite sample designated as PCH230/230, which was fabricated using filament derived from an identical melt mixing procedure to that of the PCH230/240 sample depicted in Figure 7C, it becomes evident that a printing temperature of 230°C for the composite sample is suboptimal. When the same filament was printed at 240°C printing temperature, no gap was found between the layers, and a better bond was established, and rigidity was achieved. The data obtained from the tensile test supports this conclusion.

Upon examining the 500× SEM image of the PCH250/260 composite sample as depicted in Figure 8B, it is observable that the fibers exhibit a tendency to disengage from the matrix, accompanied by surface deterioration in comparison to other samples. This phenomenon suggests that hemp fibers commence deterioration when subjected to elevated melt mixing temperatures. The observation that the sample exhibits a reduced void structure can be attributed to the influence of elevated extrusion temperatures, which are known to result in decreased void fractions.[69,70]

Upon examine Figure 9, it becomes evident that the fibers exhibit reduced damage and exhibit enhanced integration with the PC matrix, attributable to the application of a lower extrusion temperature. The gaps between the

15480569, 0, Downloaded from https://4spepublications.onlinelibrary.wiley.com/doi/10.1002/pc.28769 by Turkey Cochrane Evidence Aid, Wiley Online Library on [11/07/2024]. See the Terms and Conditions (https://onlinelibrary.wiley.com/terms-and-conditions) on Wiley Online Library for rules of use; OA articles are governed by the applicable Creative Commons License

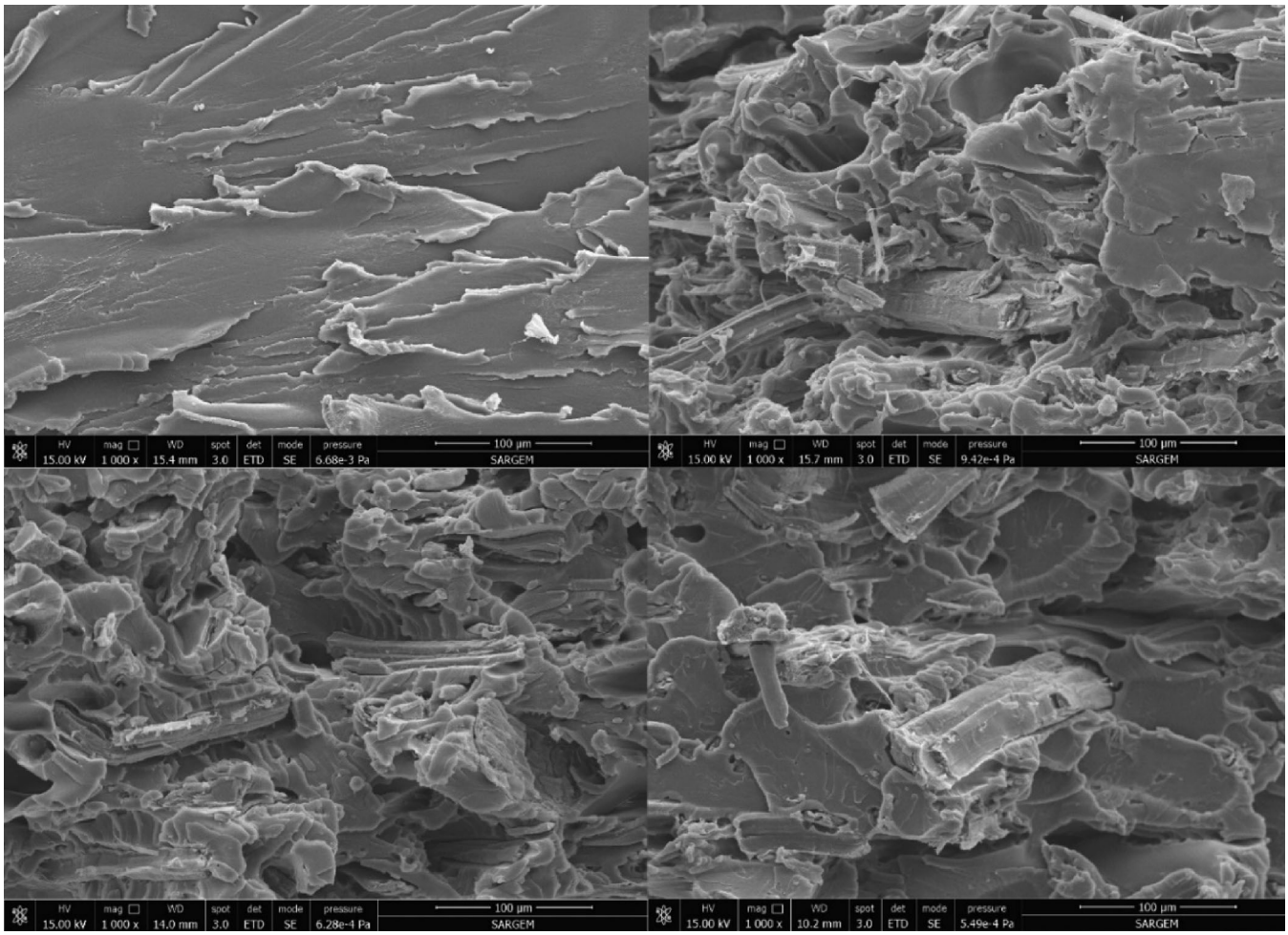


FIGURE 9 1000× SEM images. (A) Pure PC; (B) PCH250/260; (C) PCH230/240; (D) PCH230/230.

fiber and matrix material are larger in the PCH250/260 sample. In the PCH230/240 and PCH230/230 samples, where the gap between the fiber and the matrix is less, this is supported by the tensile test results that the fibers increase the mechanical properties by acting as a bridge. Higher nozzle temperatures lead to smaller partial neck growth voids.[69–71] The SEM images show that the voids in the PCH230/240 sample, produced at a higher printer temperature than the PCH230/230 sample, are more homogeneous and have softer lines. In addition, the breaking moment of the PCH230/240 composite sample is sharper, softer, and tends to elongate. As a result, for PC composite reinforced with hemp fiber, the fibers must remain intact during the melt mixing stage. Simultaneously, filament production must be carried out at a temperature where the polymer melts ensuring good mixing. In the 3Dp stage, a sufficiently high nozzle temperature must ensure interlayer adhesion. As a result, it was determined that the melt mixing temperature, which is low enough not to burn the fibers, is 230°C, and the optimum 3Dp temperature, which is high enough to stick and reduce gaps between layers, is 240°C. These results are supported by the thermal and mechanical tests.

4 | CONCLUSIONS

In this article, to contribute to sustainable architecture, the optimum melt mixing and 3D printer temperature conditions of the PC composite, which has been made partially biodegradable by adding alkaline-treated hemp fiber and can be formed with a 3Dp for architectural applications, have been investigated. To determine under which conditions the best thermal and mechanical properties of composites were achieved, they were characterized by TGA, DSC, tensile test, and SEM. According to the results, the melt mixing temperature at which hemp fiber and polymer matrix had the best thermal properties was determined to be 230°C. According to the TGA results, there was no significant decrease in the thermal properties of the filament produced by melt mixing at 230°C compared with pure PC. When we look at the

15480569, 0, Downloaded from https://4spepublications.onlinelibrary.wiley.com/doi/10.1002/pc.28769 by Turkey Cochrane Evidence Aid, Wiley Online Library on [11/07/2024]. See the Terms and Conditions (https://onlinelibrary.wiley.com/terms-and-conditions) on Wiley Online Library for rules of use; OA articles are governed by the applicable Creative Commons License

temperatures at which weight losses occur, it is observed that for PCH230, 10% weight loss occurred at 431.40°C and 50% weight loss occurred at 494.47°C. As the extruder and printing temperatures increases, it is thought that color differences occur as degradation occurs in the fibers. The T_g values obtained from the DSC analysis determined that the pure PC sample could be processed at 148.44°C, PCH250 at 148.99°C, and PCH230 at 148.64°C. No significant increase was observed in the composite samples.

Considered the tensile test values, it was determined that the samples printed on the 3Dp from filaments produced at 230°C generally had better tensile strength and Young's modulus values than those printed at 250°C. The sample with the best mechanical strength was the PCH230/240 sample with 230°C melt mixing and 240°C printing temperature. The reason for this, as supported by the SEM images, is that while the fibers remain in good condition due to the low temperature in the melt mixing stage, a sufficiently high temperature is applied to the layers to stick together in the 3Dp stage.

The tensile strength and Young's modulus values of the PCH230/240 composite were increased 12% and 29%, respectively, compared to pure PC, and not much decrease in thermal properties, the composite sample's melt mixing and 3Dp printing temperatures were considered optimum for production. The material produced within the scope of this study can be an alternative to PC material in architectural applications, as it makes PC partially biodegradable and at the same time obtains satisfactory results in both thermal and mechanical properties. In addition, because the material is suitable for use in 3D printers, complex geometric forms will be given, and freedom of design and application will be given to architecture. Thus, the potential of a material that will contribute to sustainable architecture in terms of design freedom has emerged.

ACKNOWLEDGEMENT

We thank the Kocaeli University Scientific Research Projects Coordination Unit for funding this study within the scope of "funding doctoral thesis projects." Project no: FDK-2022-2923.

DATA AVAILABILITY STATEMENT

All data have been reported in this article.

ORCID

Irem Ceylan Engin https://orcid.org/0000-0003-3761-6004
Nese Cakici Alp https://orcid.org/0000-0002-7626-9212
Ayse Aytac https://orcid.org/0000-0002-9566-7881

REFERENCES

1. Lányi E. The basic principles of sustainable architecture. *Period Polytech Arch*. 2008;38(2):79-81. doi:10.3311/pp.ar.2007-2.06
2. Sippach T, Dahy H, Uhlig K, Grisin B, Carosella S, Middendorf P. Structural optimization through biomimetic-inspired material-specific application of plant-based natural fiber-reinforced polymer composites (NFRP) for future sustainable lightweight architecture. *Polymers*. 2020;12(12):3048. doi:10.3390/polym12123048
3. Correia JR, Almeida NM, Figueira JR. Recycling of FRP composites: reusing fine GFRP waste in concrete mixtures. *J Clean Prod*. 2011;19(15):1745-1753. doi:10.1016/j.jclepro.2011.05.018
4. Kidalova L, Stevulova N, Terpakova E, Sicakova A. Utilization of alternative materials in lightweight composites. *J Clean Prod*. 2012;34:116-119. doi:10.1016/j.jclepro.2012.01.031
5. Dahy H, Petrs J, Baszynski P. Biocomposites from annually renewable resources displaying vision of future sustainable architecture. *Fabricate 2020*. UCL Press; 2020:66-73. doi:10.2307/j.ctv13xpsvw.13
6. Rihaczek G, Klammer M, Başnak O, et al. Curved foldable tailored fiber reinforcements for moldless customized biocomposite structures. Proof of concept: biomimetic NFRP stools. *Polymers*. 2020;12(9):2000. doi:10.3390/polym12092000
7. Hoogendoorn M, Blok A, Teuffel R. Bio-based composite pedestrian bridge. Part 2: materials and production process. Proceedings of the IASS Annual Symposium. 2016.
8. Dahy H. Towards sustainable buildings with free-form geometries: development and application of flexible NFRP in load-bearing structures. In Biocomposite Materials: Hameed Sultan MT, Majid MSA, Jamir MRM, Azmi AI, Saba N, (Eds). *Design and Mechanical Properties Characterization. Composites Science and Technology*, Springer, Singapore 2021;31-43. doi:10.1007/978-981-33-4091-6_2
9. Pozo Morales A, Güemes A, Fernandez-Lopez A, Carcelen Valero V, De La Rosa Llano S. Bamboo-polylactic acid (PLA) composite material for structural applications. *Materials*. 2017;10(11):1286. doi:10.3390/ma10111286
10. Tezara C, Hadi AE, Siregar JP, et al. The effect of hybridisation on mechanical properties and water absorption behaviour of woven jute/ramie reinforced epoxy composites. *Polymers (Basel)*. 2021;13(17):2964. doi:10.3390/polym13172964
11. Džalto J, Medina LA, Mitschang P. Processing of high performance biocomposites for the use in the European building industry. 20th International Conference on Composite Materials. 2015.
12. Nambiyanna B, Bakash MA, Reddy HNJ, Prabhakara R. Experimental investigation on flexural strengthening of RC slabs using natural fiber reinforced polymer composites (NFRPC). *Asian J Civ Eng*. 2021;22(8):1581-1593. doi:10.1007/s42107-021-00398-5
13. Dahy H. Materials as a design tool' design philosophy applied in three innovative research pavilions out of sustainable building materials with controlled end-of-life scenarios. *Buildings*. 2019;9(3):64. doi:10.3390/buildings9030064
14. Campbell T, Williams CB, Ivanova O. Could 3D printing change the world? Technologies, potential, and implications of additive manufacturing. *Atlantic Council*. 2011;3(1):18.

15480569, 0, Downloaded from https://4spepublications.onlinelibrary.wiley.com/doi/10.1002/pc.28769 by Turkey Cochrane Evidence Aid, Wiley Online Library on [11/07/2024]. See the Terms and Conditions (https://onlinelibrary.wiley.com/terms-and-conditions) on Wiley Online Library for rules of use; OA articles are governed by the applicable Creative Commons License

15. Guo N, Leu MC. Additive manufacturing: technology, applications and research needs. *Front Mech Eng*. 2013;8(3):215-243. doi:10.1007/s11465-013-0248-8
16. Zhao DX, Cai X, Shou GZ, Gu YQ, Wang PX. Study on the preparation of bamboo plastic composite intend for additive manufacturing. *Key Eng Mater*. 2015;667:250-258.
17. Tran TN, Bayer IS, Heredia-Guerrero JA, et al. Cocoa shell waste biofilaments for 3D printing applications. *Macromol Mater Eng*. 2017;302(11):1700219. doi:10.1002/mame.201700219
18. Mazzanti V, Malagutti L, Mollica F. FDM 3D printing of polymers containing natural fillers: a review of their mechanical properties. *Polymers*. 2019;11(7):1094. doi:10.3390/polym11071094
19. Perkins I, Skitmore M. Three-dimensional printing in the construction industry: a review. *Int J Constr Manag*. 2015;15(1):1-9. doi:10.1080/15623599.2015.1012136
20. Marijnissen MPAM, Van Der Zee A. 3D concrete printing in architecture a research on the potential benefits of 3D concrete printing in architecture. *Mater Stud Methodol*. 2017;2:299-308.
21. Siddika A, Mamun MA, Al, Ferdous W, Saha AK, Alyousef R. 3D-printed concrete: applications, performance, and challenges. *J Sustain Cem Based Mater*. 2020;9(3):127-164. doi:10.1080/21650373.2019.1705199
22. Morán J, Alvarez V, Petrucci R, Kenny J, Vazquez A. Mechanical properties of polypropylene composites based on natural fibers subjected to multiple extrusion cycles. *J Appl Polym Sci*. 2007;103(1):228-237. doi:10.1002/app.25173
23. Osman MA, Atia MRA. Investigation of ABS-rice straw composite feedstock filament for FDM. *Rapid Prototyp J*. 2018;24(6):1067-1075. doi:10.1108/RPJ-11-2017-0242
24. McIlroy C, Olmsted PD. Disentanglement effects on welding behaviour of polymer melts during the fused-filament-fabrication method for additive manufacturing. *Polymers*. 2017;123:376-391. doi:10.1016/j.polymer.2017.06.051
25. Mohan N, Senthil P, Vinodh S, Jayanth N. A review on composite materials and process parameters optimisation for the fused deposition modelling process. *Virtual Phys Prototyp*. 2017;12(1):47-59. doi:10.1080/17452759.2016.1274490
26. Rosa SML, Santos EF, Ferreira CA, Nachtigall SMB. Studies on the properties of rice-husk-filled-PP composites: effect of maleated PP. *Mat Res*. 2009;12(3):333-338. doi:10.1590/S1516-14392009000300014
27. Kochesfahani SH. Improving PLA-based material for 3-D printers using fused deposition modeling. *Plast Eng*. 2016;72(5):36-43. doi:10.1002/j.1941-9635.2016.tb01538.x
28. Depuydt D, Balthazar M, Hendrickx K, et al. Production and characterization of bamboo and flax fiber reinforced polylactic acid filaments for fused deposition modeling (FDM). *Polym Compos*. 2019;40(5):1951-1963. doi:10.1002/pc.24971
29. Torrado AR, Shemelya CM, English JD, Lin Y, Wicker RB, Roberson DA. Characterizing the effect of additives to ABS on the mechanical property anisotropy of specimens fabricated by material extrusion 3D printing. *Addit Manuf*. 2015;6:16-29. doi:10.1016/j.addma.2015.02.001
30. Torrado Perez AR, Roberson DA, Wicker RB. Fracture surface analysis of 3D-printed tensile specimens of novel ABS-based materials. *JFAP*. 2014;14(3):343-353. doi:10.1007/s11668-014-9803-9
31. Appusamy AM, Nanjappan N, Eswaran P, Subramanian M. The effect of natural Gongura roselle fiber on the mechanical properties of 3D printed ABS and PLA composites. *Polimery*. 2022;67(3):119-124. doi:10.14314/polimery.2022.3.4
32. Šafka J, Ackermann M, Bobek J, Seidl M, Habr J, Běhálek L. Use of composite materials for FDM 3D print technology. *Mater Sci Forum*. 2016;862:174-181.
33. Ahmad MN, Wahid MK, Maidin NA, Ab Rahman MH, Osman MH, Alis Elias IF. Mechanical characteristics of oil palm fiber reinforced thermoplastics as filament for fused deposition modeling (FDM). *Adv Manuf*. 2020;8(1):72-81. doi:10.1007/s40436-019-00287-w
34. Marton AMS, Monticeli FM, Zanini NC, et al. Revalorization of Australian royal palm (Archontophoenix alexandrae) waste as reinforcement in acrylonitrile butadiene styrene (ABS) for use in 3D printing pen. *J Clean Prod*. 2022;365:132808. doi:10.1016/j.jclepro.2022.132808
35. Matsuzaki R, Ueda M, Namiki M, et al. Three-dimensional printing of continuous-fiber composites by in-nozzle impregnation. *Sci Rep*. 2016;6(1):23058. doi:10.1038/srep23058
36. Agaliotis EM, Ake-Concha BD, May-Pat A, et al. Tensile behavior of 3D printed polylactic acid (PLA) based composites reinforced with natural fiber. *Polymers*. 2022;14(19):3976. doi:10.3390/polym14193976
37. Figueroa-Velarde V, Diaz-Vidal T, Cisneros-López EO, et al. Mechanical and physicochemical properties of 3D-printed agave fibers/poly(lactic) acid biocomposites. *Materials*. 2021;14(11):3111. doi:10.3390/ma14113111
38. Liu H, He H, Peng X, Huang B, Li J. Three-dimensional printing of poly(lactic acid) bio-based composites with sugarcane bagasse fiber: effect of printing orientation on tensile performance. *Polym Adv Technol*. 2019;30(4):910-922. doi:10.1002/pat.4524
39. Stoof D, Pickering K, Zhang Y. Fused deposition modelling of natural fibre/polylactic acid composites. *J Compos Sci*. 2017;1(1):8. doi:10.3390/jcs1010008
40. Oksman K, Skrifvars M, Selin JF. Natural fibres as reinforcement in polylactic acid (PLA) composites. *Compos Sci Technol*. 2003;63(9):1317-1324. doi:10.1016/S0266-3538(03)00103-9
41. Milosevic M, Stoof D, Pickering K. Characterizing the mechanical properties of fused deposition modelling natural fiber recycled polypropylene composites. *J Compos Sci*. 2017;1(1):7. doi:10.3390/jcs1010007
42. Stoof D, Pickering K. Sustainable composite fused deposition modelling filament using recycled pre-consumer polypropylene. *Compos B Eng*. 2018;135:110-118. doi:10.1016/j.compositesb.2017.10.005
43. Badouard C, Traon F, Denoual C, Mayer-Laigle C, Païs G, Bourmaud A. Exploring mechanical properties of fully compostable flax reinforced composite filaments for 3D printing applications. *Ind Crops Prod*. 2019;135:246-250. doi:10.1016/j.indcrop.2019.04.049
44. Dönitz A, Köllner A, Richter T, Löschke O, Auhl D, Völlmecke C. Additive manufacturing of biodegradable hemp-reinforced polybutylene succinate (PBS) and its mechanical characterization. *Polymers*. 2023;15(10):2271. doi:10.3390/polym15102271
45. Inseemeesak B, Siripaiboon C, Somkeattikul K, et al. Biocomposite fabrication from pilot-scale steam-exploded coconut fiber

15480569, 0, Downloaded from https://4spepublications.onlinelibrary.wiley.com/doi/10.1002/pc.28769 by Turkey Cochrane Evidence Aid, Wiley Online Library on [11/07/2024]. See the Terms and Conditions (https://onlinelibrary.wiley.com/terms-and-conditions) on Wiley Online Library for rules of use; OA articles are governed by the applicable Creative Commons License

and PLA/PBS with mechanical and thermal characterizations. *J Clean Prod*. 2022;379:134517. doi:10.1016/j.jclepro.2022.134517

46. Ariel Leong JJ, Koay SC, Chan MY, Choo HL, Tshai KY, Ong TK. Composite filament made from post-used Styrofoam and corn husk fiber for fuse deposition modeling. *J Nat Fibers*. 2022;19(13):7033-7048. doi:10.1080/15440478.2021.1941488
47. Dudek P. FDM 3D printing technology in manufacturing composite elements. *AMM*. 2013;58(4):1415-1418. doi:10.2478/amm-2013-0186
48. Deb D, Jafferson JM. Natural fibers reinforced FDM 3D printing filaments. *Mater Today Proc*. 2021;46:1308-1318. doi:10.1016/j.matpr.2021.02.397
49. Defoirdt N, Biswas S, Vriese LD, et al. Assessment of the tensile properties of coir, bamboo and jute fibre. *Compos Part A Appl Sci Manuf*. 2010;41(5):588-595. doi:10.1016/j.compositesa.2010.01.005
50. le Duigou A, Bourmaud A, Balnois E, Davies P, Baley C. Improving the interfacial properties between flax fibres and PLLA by a water fibre treatment and drying cycle. *Ind Crops Prod*. 2012;39:31-39. doi:10.1016/j.indcrop.2012.02.001
51. Le Duigou A, Correa D, Ueda M, Matsuzaki R, Castro M. A review of 3D and 4D printing of natural fibre biocomposites. *Mater Des*. 2020;194:108911. doi:10.1016/j.matdes.2020.108911
52. Amaducci S, Scordia D, Liu FH, et al. Key cultivation techniques for hemp in Europe and China. *Ind Crops Prod*. 2015;68:2-16. doi:10.1016/j.indcrop.2014.06.041
53. Ceylan İ, Çakıcı Alp N, Aytaç A. Sustainable 3D printing with alkali-treated hemp fiber-reinforced polycarbonate composites. *Cellulose*. 2024;31(7):4477-4495. doi:10.1007/s10570-024-05904-x
54. Liu M, Thygesen A, Summerscales J, Meyer AS. Targeted pre-treatment of hemp bast fibres for optimal performance in biocomposite materials: a review. *Ind Crops Prod*. 2017;108:660-683. doi:10.1016/j.indcrop.2017.07.027
55. Marrot L, Lefeuvre A, Pontoire B, Bourmaud A, Baley C. Analysis of the hemp fiber mechanical properties and their scattering (fedora 17). *Ind Crops Prod*. 2013;51:317-327. doi:10.1016/j.indcrop.2013.09.026
56. Liu H, You L, Jin H, Yu W. Influence of alkali treatment on the structure and properties of hemp fibers. *Fibers Polym*. 2013;14(3):389-395. doi:10.1007/s12221-013-0389-8
57. Shah I, Jing L, Fei ZM, Yuan YS, Farooq MU, Kanjana N. A review on chemical modification by using sodium hydroxide (NaOH) to investigate the mechanical properties of sisal, coir and hemp fiber reinforced concrete composites. *J Nat Fibers*. 2022;19(13):5133-5151. doi:10.1080/15440478.2021.1875359
58. Suardana NPG, Piao Y, Lim JK. Mechanical properties of hemp fibers and hemp/PP composites: effects of chemical surface treatment. *Mater Phys Mech*. 2011;11(1):1-8.
59. Rachini A, Le Troedec M, Peyratout C, Smith A. Comparison of the thermal degradation of natural, alkali-treated and silane-treated hemp fibers under air and an inert atmosphere. *J Appl Polym Sci*. 2009;112(1):226-234. doi:10.1002/app.29412
60. Bhoopathi R, Ramesh M. Influence of eggshell nanoparticles and effect of alkalization on characterization of industrial hemp fibre reinforced epoxy composites. *J Polym Environ*. 2020;28(8):2178-2190. doi:10.1007/s10924-020-01756-1
61. Dayo AQ, Gao BC, Wang J, et al. Natural hemp fiber reinforced polybenzoxazine composites: curing behavior, mechanical and thermal properties. *Compos Sci Technol*. 2017;144:114-124. doi:10.1016/j.compscitech.2017.03.024
62. Stelea L, Filip I, Lisa G, et al. Characterisation of hemp fibres reinforced composites using thermoplastic polymers as matrices. *Polymers (Basel)*. 2022;14(3):481. doi:10.3390/polym14030481
63. Oza S, Ning H, Ferguson I, Lu N. Effect of surface treatment on thermal stability of the hemp-PLA composites: correlation of activation energy with thermal degradation. *Compos B Eng*. 2014;67:227-232. doi:10.1016/j.compositesb.2014.06.033
64. Maheswari CU, Reddy KO, Muzenda E, Rajulu AV. Tensile and thermal properties of polycarbonate-coated tamarind fruit fibers. *Int J Polym Anal Charact*. 2012;17(8):578-589. doi:10.1080/1023666X.2012.718527
65. Threepopnatkul P, Kaerkitcha N, Athipongarporn N. Effect of surface treatment on performance of pineapple leaf fiber–polycarbonate composites. *Compos B Eng*. 2009;40(7):628-632. doi:10.1016/j.compositesb.2009.04.008
66. Baghaei B, Skrifvars M, Rissanen M, Ramamoorthy SK. Mechanical and thermal characterization of compression moulded polylactic acid natural fiber composites reinforced with hemp and lyocell fibers. *J Appl Polym Sci*. 2014;131(15):40534. doi:10.1002/app.40534
67. Karsli NG, Aytac A. Properties of alkali treated short flax fiber reinforced poly(lactic acid)/polycarbonate composites. *Fibers Polym*. 2014;15(12):2607-2612. doi:10.1007/s12221-014-2607-4
68. Zhou Y, Zou J, Wu H, Xu B. Balance between bonding and deposition during fused deposition modeling of polycarbonate and acrylonitrile-butadiene-styrene composites. *Polym Compos*. 2020;41(1):60-72. doi:10.1002/pc.25345
69. Wang L, Gardner DJ. Effect of fused layer modeling (FLM) processing parameters on impact strength of cellular polypropylene. *Polymers*. 2017;113:74-80. doi:10.1016/j.polymer.2017.02.055
70. Tao Y, Kong F, Li Z, et al. A review on voids of 3D printed parts by fused filament fabrication. *J Mater Res Technol*. 2021;15:4860-4879. doi:10.1016/j.jmrt.2021.10.108
71. Aliheidari N, Christ J, Tripuraneni R, Nadimpalli S, Ameli A. Interlayer adhesion and fracture resistance of polymers printed through melt extrusion additive manufacturing process. *Mater Des*. 2018;156:351-361. doi:10.1016/j.matdes.2018.07.001

How to cite this article: Ceylan Engin I, Cakici Alp N, Aytac A. Determination of optimum production and 3D printer application temperatures for hemp fiber reinforced polycarbonate composites. *Polym Compos*. 2024; 1-14. doi:10.1002/pc.28769

15480569, 0, Downloaded from https://4spepublications.onlinelibrary.wiley.com/doi/10.1002/pc.28769 by Turkey Cochrane Evidence Aid, Wiley Online Library on [11/07/2024]. See the Terms and Conditions (https://onlinelibrary.wiley.com/terms-and-conditions) on Wiley Online Library for rules of use; OA articles are governed by the applicable Creative Commons License